

キセノン原子のサブドップラー二光子励起スペクトルにみられる  
微細構造と同位体シフト

(豪州国立大<sup>1</sup>, Macquarie大<sup>2</sup>, 関学千里国際<sup>3</sup>) ◦河野光彦<sup>1,3</sup>, He Yabai<sup>2</sup>, Orr Brian<sup>2</sup>, Baldwin Kenneth<sup>1</sup>

Hyperfine structure and isotope shifts in sub-Doppler two-photon-excitation  
Rydberg spectra of xenon

(ANU<sup>1</sup>, Macquarie Univ<sup>2</sup>, SOIS<sup>3</sup>) ◦Mitsuhiko Kono<sup>1,3</sup>, Yabai He<sup>2</sup>, Brian J Orr<sup>2</sup>, Kenneth G H Baldwin<sup>1</sup>

### 1. Introduction

We have observed high-resolution spectra concerning two-photon transitions of xenon (Xe) from the  $5p^6 \ ^1S_0$  ground state to 33 high-energy Rydberg levels ranging from 97300 to 94100  $\text{cm}^{-1}$ . Diverse hyperfine-structure (hfs) and isotope-shift effects are revealed in the atomic spectra that are recorded in these experiments. The spectra also provide performance tests for a versatile high-performance all-solid-state coherent tunable ultraviolet (UV) light source ranging from 205 to 213 nm that has been developed to improve the accuracy of a previous determination [1] of the absolute frequency for the  $1 \ ^1S \rightarrow 2 \ ^1S$  two-photon transition of helium (He). The Lamb shift in ground-state He is a significant test of quantum-electrodynamic theory. We have previously used this instrument for two-photon excitation (TPE) spectroscopy of atoms such as cesium at  $\sim 822.5$  nm [2] and krypton at  $\sim 212.5$  nm [3]. Many earlier experiments on isotope energy shifts in Xe include a sub-Doppler TPE study of its  $5p^6 \rightarrow 5p^5 6p$  transitions [4]. The energetics of Xe and its ions has been surveyed [5]. Analysis of the observed sub-Doppler atomic spectra in the present study yields isotope energy shifts and (for 28 of the 33 Rydberg levels) associated hyperfine structure (hfs), which has only rarely been resolved at optical excitation energies as high as 94 000  $\text{cm}^{-1}$  [6].

### 2. Experimental

Tunable SLM coherent light pulses are generated by a chirp-controllable pulsed optical parametric oscillator (OPO) based on a periodically poled  $\text{KTiOPO}_4$  crystal in a compact ring cavity. The OPO is injection-seeded by a cw Ti:sapphire ring laser and pumped at 532 nm by long-duration pulsed radiation from a Nd:YAG laser. A multipass Ti:sapphire amplifier system boosts the OPO output pulse energy to  $\sim 45$  mJ. NLO upconversion of fundamental optical pulses at 820–850 nm then yield  $\sim 1$  mJ of tunable pulsed coherent UV light at 205–213 nm, with a transform-limited spectral bandwidth of  $\sim 100$  MHz [3,6]. The UV pulsed beam enters an ionization cell containing a sample gas of pure Xe at room temperature and 0.10 Torr (0.13 mbar); these conditions avoid signal saturation and pressure broadening. The UV beam is expanded, collimated, and retro-reflected back through the ionization cell. This counter-propagating optical geometry yields sub-Doppler TPE spectra of the Xe atoms, with the ionization signal recorded by means of a 36-volt biased electrode and gated boxcar integrator.

### 3. Results and discussion

Our TPE spectra entail resonant excitation of a  $5p$  electron from the  $5s^2 5p^6$  valence shell of Xe (which corresponds to its  $^1S_0$  ground level) to Rydberg levels. Two representative examples (each with angular momentum quantum number  $J > 0$  and therefore exhibiting hyperfine splitting) are shown in Fig 1. The assorted TPE spectra depend subtly on the respective contributions of the isotopes of Xe, of which the six most prominent (with natural isotopic abundances) are:  $^{132}\text{Xe}$  (26.9%),  $^{129}\text{Xe}$  (26.4%),  $^{131}\text{Xe}$  (21.2%),  $^{134}\text{Xe}$  (10.4%),  $^{136}\text{Xe}$  (8.9%), and  $^{130}\text{Xe}$  (4.1%). Xe has only two stable magnetic isotopes with non-zero nuclear spin  $I$  and the possibility of hyperfine splitting, namely:  $^{129}\text{Xe}$  ( $I = 1/2$ ) and  $^{131}\text{Xe}$  ( $I = 3/2$ ). Least-squares fits to isotope energy shifts for  $I = 0$  isotopes and/or levels with  $J = 0$  are referenced to the  $6p [1/2]_0$  transition [4] at a TPE energy of  $\sim 80\,119 \text{ cm}^{-1}$  [5], via a scaling factor  $PSF$ . The spectra of two stable magnetic isotopes,  $^{129}\text{Xe}$

( $I = 1/2$ ) and  $^{131}\text{Xe}$  ( $I = 3/2$ ), exhibit hfs (apart from  $J = 0$  levels), depending on coupling parameters,  $A^{129}$  and  $A^{131}$  (both magnetic-dipole) and  $B^{131}$  (electric-quadrupole). Parameters that are needed to fit our 33 Rydberg levels of Xe are summarised in Table 1, where numerical values are averages for unconstrained least-squares fits to our spectra for each of five sets of Xe Rydberg levels.

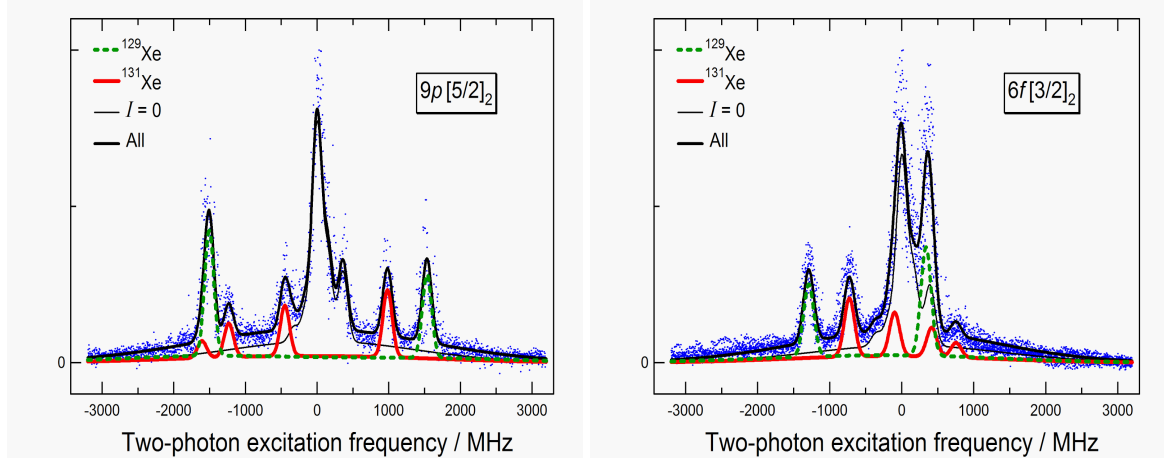


**Fig. 1.** Sub-Doppler two-photon excitation spectra for Xe  $5p^6\ ^1S_0 \rightarrow 5p^5\ 9p[5/2]_2$  (left panel) and Xe  $5p^6\ ^1S_0 \rightarrow 5p^5\ 6f[3/2]_2$  (right panel) transitions, with the UV wavelengths at  $\sim 212.5$  nm and  $\sim 211.1$  nm, respectively. Their origins arbitrarily are set at the  $^{132}\text{Xe}$ -isotope peaks. The solid red trace is a simulated curve of best fit to the blue experimental data points, as explained in the text.

In ongoing research, we have adapted the atomic-beam apparatus employed previously in early experiments on the  $1\ ^1S \rightarrow 2\ ^1S$  TPE transition in He [1]. This provides isotopic mass selectivity to distinguish spectral contributions from individual Xe isotopes and thereby to resolve some of the heavily overlapped spectra that were previously recorded in natural isotopic abundance [6]. This approach is expected to help to reduce the uncertainties, particularly for the  $nf\ [5/2]_2$  ( $n = 6-10$ ) levels where remarkably small hyperfine coupling parameters  $A^{129}$  and  $A^{131}$  are found and best-fit values of  $B^{131}$  are ambiguous [6].

**Table 1.** Isotope-shift and hfs fits for 33 Rydberg levels of Xe

Excited Xe Rydberg levels	Scaling factor $PSF$	$A^{129}$ / MHz †	$B^{131}$ / MHz
$np\ [1/2]_0$ ( $n = 9-13$ )	$1.16 \pm 0.03$	(no hfs for $J = 0$ levels)	
$np\ [3/2]_2$ ( $n = 9-13$ )	$1.16 \pm 0.02$	$-828 \pm 13$	$-21 \pm 12$
$nf\ [3/2]_2$ ( $n = 6-14$ )	$1.24 \pm 0.09$	$644 \pm 25$	$48 \pm 52$
$np\ [5/2]_2$ ( $n = 9-17$ )	$1.20 \pm 0.09$	$-1205 \pm 11$	$210 \pm 42$
$nf\ [5/2]_2$ ( $n = 6-10$ )	$1.17_5 \pm 0.09$	$0 \pm 50$	$\pm (150 \pm 100)$

† Theoretically predicted value of  $(A^{129} / A^{131}) = -3.3734$

We acknowledge support from the Australian Research Council.

#### 4. References

- [1] S.D. Bergeson, *et al.*, *Phys. Rev. Lett.* **80**, 3475–3478 (1998); S.D. Bergeson, *et al.*, *Physica Scripta* **T83** 76–82 (1999); S.D. Bergeson, *et al.*, *J. Opt. Soc. Am. B* **17**, 1599–1606 (2000).
- [2] M. Kono, K.G.H. Baldwin, Y. He, R.T. White, and B.J. Orr, *Opt. Lett.* **30**, 3413–3415 (2005); *J. Opt. Soc. Am. B* **23**, 1181–1189 (2006).
- [3] Y. He, M. Kono, R.T. White, M.J. Sellars, K.G.H. Baldwin, and B.J. Orr, *Appl. Phys. B* **99**, 609–612 (2010).
- [4] M.D. Plimmer, P.E.G. Baird, C.J. Foot, D.N. Stacey, J.B. Swan, and G.K. Woodgate, *J. Phys. B* **22**, L241 (1989).
- [5] E.B. Saloman, *J. Phys. Chem. Ref. Data* **33** 765–921 (2004).
- [6] M. Kono, Y. He, K.G.H. Baldwin, R.T. White, and B.J. Orr, *J. Phys. B: At. Mol. Opt. Phys.* **46**, 035401 (2013).